# 6

# Rheology: Tools and Methods

**Saad A. Khan, Joseph R. Royer, and Srinivasa R. Raghavan**
**Department of Chemical Engineering**
**North Carolina State University**

## INTRODUCTION

In this paper, we attempt to give the reader a basic understanding of rheology, a scientific discipline of great utility in characterizing complex, microstructured media. Rheology is formally defined as the study of deformation and flow behavior in various materials (Macosko, 1994). Since its humble origins in the 1920s in the laboratories of Eugene Bingham at Lehigh University, rheology has developed into a mature field of wide-ranging applicability.

Systems investigated using rheology can typically be classified as soft condensed matter or as complex fluids. Examples include macromolecular systems, such as polymer melts and solutions, gels, and biological fluids, as well as colloidal and multiphase systems, such as dispersions, emulsions, foams, and surfactant solutions. Typically, these materials are *viscoelastic,* i.e. they exhibit a combination of viscous and elastic properties. Such complex behavior cannot be characterized purely in terms of simple parameters, such as the material viscosity or elastic modulus.

One of the objectives of this paper is to indicate the possible applications of rheology towards designing improved aviation fuels. Although an aviation fuel typically behaves like a viscous liquid, the introduction of certain additives can cause the system to show a viscoelastic response (Hoyt et al., 1980). In that case, the rheology of the system becomes important, and rheological studies will be necessary for accurately modeling the flow in the aircraft engine. Moreover, it is possible that a controlled amount of viscoelasticity may prove to be beneficial to the overall performance of the aviation fuel. For instance, the addition of an "antimisting" component to the fuel can reduce the fire hazard in case of a fuel leak (Chao et al., 1984).

Our agenda for this paper is ambitious: we would like to cover the most important rheological principles, techniques, and methods, as well as indicate specific applications—all within about 20 pages. Clearly, we have to be very selective in the topics we choose to describe. Our focus will be on reviewing the material parameters obtained using rheology and the correlation of these parameters to material microstructure. In this context, the *microstructure* implies the spatial disposition of molecules, particles, or other entities in the system over length scales on the order of microns (Barnes, 1993). We will consider the three most common kinds of rheological techniques, viz. steady-shear rheology, dynamic rheology, and extensional rheology. We will then provide some specific examples for the applications of rheology to materials characterization and design. For the interested reader, we have supplied an extensive list of references for obtaining more detailed information on various aspects of rheology as well as on specialized rheological methods.

## VISCOELASTIC BEHAVIOR

The science of rheology attempts to bridge the gap between solid mechanics (which deals with perfectly elastic solids) and fluid mechanics (which deals with perfectly viscous liquids). Thus, the rheologist is typically interested in viscoelastic systems that exhibit a combination of elastic and viscous behavior. To understand viscoelasticity, it will be helpful to consider first the cases of perfect elasticity or viscosity, which can be interpreted in terms of simple relationships such as Hooke's law for solids and Newton's law for liquids, respectively. We will now consider these two laws and indicate their applicability, or lack thereof, for various materials.

Fundamental relationships linking force and material deformation are called constitutive equations (Bird et al., 1987). For an elastic solid, the *constitutive equation* is Hooke's law, which states that the applied shear-stress ($\tau$) is proportional to the produced shear-strain ($\gamma$) or alternately:

$$\tau = G\gamma \tag{1}$$

Here, the shear-stress ($\tau$) is the shear force per unit area, and the strain ($\gamma$) is defined as the relative change in length. The proportionality constant ($G$) is called the shear modulus

and is an intrinsic property of an elastic solid. For Hookean solids when the stress is removed, the strain becomes zero and the material regains its original shape and structure. Thus, the elasticity of a material represents its ability to regain its shape and structure after deformation, i.e., to store deformation energy. Most metals and ceramics obey Hooke's law at small strains.

A similar constitutive equation exists for a viscous or Newtonian liquid. Newton's law of viscosity states that the shear stress ($\tau$) is proportional to the rate of strain, or shear rate ($\dot{\gamma}$).

$$\tau=\eta\dot{\gamma} \qquad (2)$$

The proportionality constant ($\eta$) is defined as the viscosity of the material. Thus, a Newtonian liquid will undergo a constant rate of deformation under an applied stress, and when the stress is removed it will remain in the shape and structure it has adopted. The viscosity of a material is a measure of its internal resistance to flow and reflects the rate at which energy is dissipated in the material. Many small-molecule liquids, such as water, honey, and various oils, obey Newton's law.

As we have indicated, there are several materials that obey these constitutive equations. These materials can be completely characterized by measuring the respective parameters, $G$ or $\eta$. But in reality, many systems, such as colloids, polymers, and gels, do not obey these simple constitutive relations. Instead, these materials have properties between those of a Hookean solid and a Newtonian liquid and can be classified as non-Newtonian or viscoelastic. For these materials, the viscosity is a function of shear-rate and, hence, not constant, and the shear modulus has two components signifying elastic and viscous character respectively.

Many simple experiments can demonstrate viscoelastic or non-Newtonian behavior (Boger and Walters, 1993; Bird et al., 1987; Schramm, 1994). First, consider "silly putty," which is a poly(dimethyl siloxane) (PDMS) elastomer of moderate molecular weight. When a ball of silly putty is dropped onto a solid surface, it bounces back like a rubber ball, thereby behaving almost like an elastic solid. However, if the putty is placed on that same solid surface for some time, it will slowly flow under the stress of gravity, thus showing behavior characteristic of a highly viscous fluid. Therefore, silly putty can behave both like an elastic solid or a viscous liquid, depending on the time scale of the deformation.

A second example of non-Newtonian behavior is "rod climbing" (or the Weissenberg effect). When a vertical rod is rotated in a container of Newtonian fluid, such as water, the inertial forces acting on the fluid cause it to move away from the rod. This creates a situation where the fluid level at the rod is lower than the fluid level at the container walls (Figure 6-1a). If the same experiment is run in a container of polymeric fluid, the flow changes directions and moves toward the rod. This phenomenon is called rod climbing and is caused by the influence of normal stresses on flow properties (Figure 6-1b). These normal stresses create tension along the circular lines of flow and generate pressure toward the center, which drives the polymeric fluid up the rod.

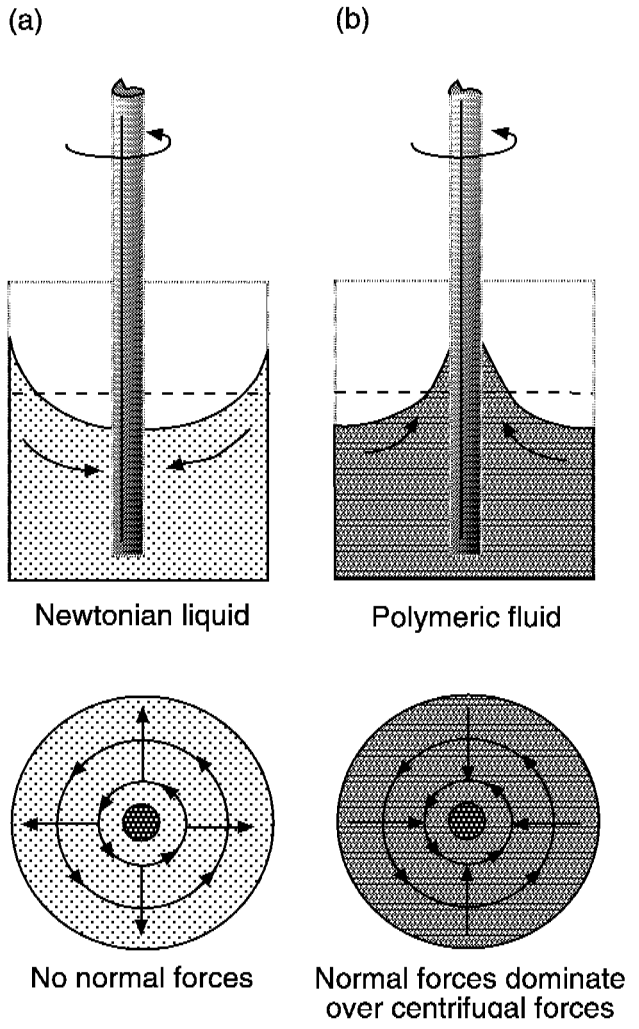


FIGURE 6-1 Rod climbing (Weissenberg effect). (a) In Newtonian fluids, centrifugal forces generated by the rotation push the fluid away from the rod. (b) In non-Newtonian fluids, normal forces are stronger than centrifugal forces and drive the fluid inward toward the rod.

Another dramatic illustration of viscoelastic effects is the "tubeless siphon" experiment. When a Newtonian liquid, such as water, is drained out of a container through a siphon, the tube must remain under the level of liquid in order for the liquid to continue to flow. However, a polymeric (non-Newtonian liquid) can continue to flow up and through the siphon even after the tube is raised above the liquid level (Figure 6-2). The fluid undergoes extensional flow (stretching) in this case, and the elastic nature of the polymeric fluid enables it to be extended upwards and sucked into the tube.

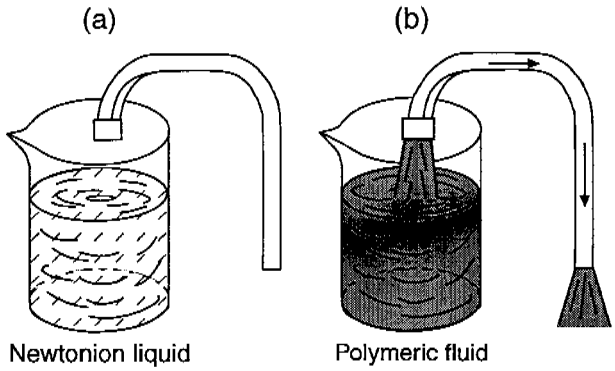


FIGURE 6-2 Tubeless siphon. (a) Newtonian fluid cannot be siphoned unless tube is below fluid level. (b) Normal stresses allow non-Newtonian fluid to be siphoned even when tube is above fluid level.

## STEADY-SHEAR RHEOLOGY

Simple steady-shear flow is the easiest flow to generate and is, therefore, of central importance in rheology. Most of the rheological data reported in the literature is for steady-shear material functions. Moreover, flows occurring in a number of industrial processes, such as extrusion or flow-through circular dies, approximate steady-shear flow.

We will try to provide a basic understanding of steady-shear flow (Bird et al., 1987). In Figure 6-3a, two parallel plates are shown, between which lies a generic fluid. Suppose that both plates are initially at rest with no flow occurring. At a time $t = 0$, the upper plate is made to instantaneously attain a constant velocity (v). This results in the generation of a shear stress ($\tau$) in the fluid from the cohesive forces between the fluid molecules. As the fluid flows, specific fluid elements (i.e., tiny packets of fluid that remain together at all times during the experiment) can be tracked as a function of time. It is easy to see that every fluid element will undergo the same strain, and that the local strain everywhere in the fluid will be equal to the overall shear strain. In the same way, the shear rate ($\dot{\gamma}$) which is the rate of change of shear strain, can be shown to be constant throughout the fluid and equal to ($v/h$). Thus, the shear rate applied on the system can be estimated from the velocity (v) applied to the top plate and the distance ($h$) between the plates.

From a steady-shear flow experiment, three material functions can be measured, viz. the viscosity ($\eta$), and the first and second normal-stress coefficients ($\Psi_1$ and $\Psi_2$). Among these, the viscosity ($\eta$) is the simplest and most important material

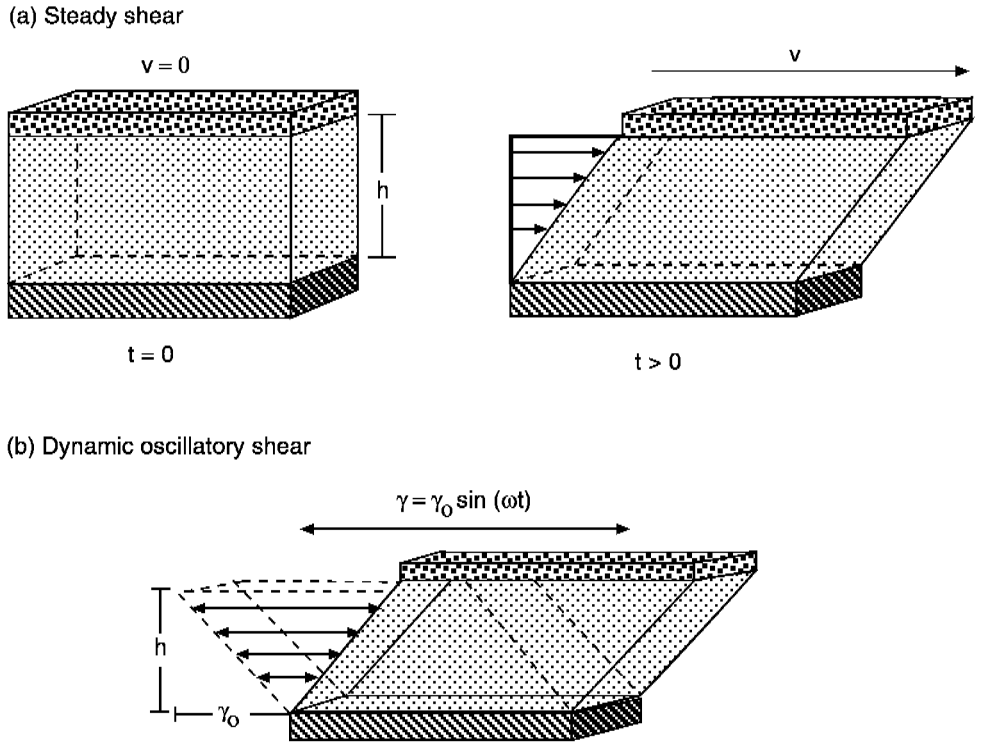


FIGURE 6-3 Two types of shear deformation. The arrows represent the velocity field in the fluid in each case. (a) Steady shear of a fluid between two parallel plates. At time $t = 0$, the system is at rest. At $t > 0$, the top plate is made to attain a constant velocity ($v$). (b) Dynamic (oscillatory) shear of a fluid between parallel plates. The top plate moves in a sinusoidal fashion with a maximum strain amplitude ($\gamma_0$).

function and can be calculated from the measured shear stress ($\tau$), and the applied shear rate ($\dot{\gamma}$) by:

$$\eta(\dot{\gamma}) = \frac{\tau(\dot{\gamma})}{\dot{\gamma}} \tag{3}$$

Note that this expression is analogous to Newton's law for simple liquids, with the caveat that the viscosity here (more properly termed the apparent viscosity) is a function of shear rate and not a constant parameter. The normal-stress coefficients ($\Psi_1$ and $\Psi_2$) are estimated in a similar manner by measuring the force per unit area exerted in directions normal to the direction of flow. However, they are much harder to measure accurately. The interested reader is referred to books by Ferry (1980) and Bird et al. (1987) for discussions of normal stresses.

Rheological experiments under steady shear are performed using "viscometric flows" that are indistinguishable from simple steady flow for all practical purposes (Dealy and Wissbrun, 1990). Thus, the three material functions that govern the behavior of the fluid ($\eta$, $\Psi_1$, and $\Psi_2$) can be obtained experimentally. Let us now examine some typical examples of material behavior under steady shear. We will focus on the most important material parameter, the steady-shear viscosity as a function of shear-rate, $\eta(\dot{\gamma})$. Four types of behavior can be distinguished: Newtonian, shear thinning, yield stress (followed usually by shear thinning), and shear thickening. The last three are all examples of non-Newtonian or viscoelastic behavior.

A plot of viscosity versus shear-rate or shear-stress is called a flow curve. It is common practice to plot the flow curve on a log-log plot as shown throughout Figure 6-4. The simplest type of steady-shear response is Newtonian behavior (Figure 6-4a), which implies a constant viscosity for the system, independent of shear rate. This is also manifested as a linear relationship between shear stress and shear rate (Newton's law), with the slope of the line defining the viscosity. Most low molecular-weight liquids and gases show Newtonian behavior.

Among non-Newtonian phenomena, the most widely observed is shear thinning, which implies a decrease in viscosity over a range of shear rates. This behavior is exhibited by most polymeric solutions and melts (Ferry, 1980), as well as by a large number of colloidal systems (Russel et al., 1989). In the simplest case, the sample shows Newtonian behavior at low shear rates and shear thinning at higher shear rates (Figure 6-4b). Thus, at low shear rates, the viscosity attains a constant value called the zero-shear viscosity ($\eta_0$). However, as the shear rate is increased, there occurs a critical shear rate ($\dot{\gamma}_c$), above which the viscosity of the sample decreases. Examples of shear thinning fluids include blood, saliva, various sauces, and creams.

Shear thinning sometimes occurs in conjunction with yield-stress behavior (Macosko, 1994). In this case, the system will not show any motion until a certain critical or yield stress ($\tau_y$) is reached. Below the yield-stress, the viscosity of the material approaches infinity (Figure 6-4c), and the system responds in a plastic-like fashion. Above the yield stress, the material typically shows shear thinning. When viscosity is plotted versus shear rate, the existence of a yield stress is reflected as a characteristic slope of –1 in the low shear rate portion of the plot (Figure 6-4c). Some materials approximate Newtonian behavior beyond the yield stress, and these materials are called viscoplastics or Bingham plastics, after Eugene Bingham who first described paint this way in the 1920s. Materials that show a yield-stress appear to have a solid-like consistency when at rest, but when stirred or agitated, they can be made to flow quite easily. Food substances, such as mayonnaise, ketchup, and salad dressing, are good examples.

Modeling the steady-shear response has been a constant endeavor for rheologists. Several models have been formulated, particularly for shear thinning and yield-stress behavior. We will only mention two of the simplest and most convenient models. For shear thinning, the power-law model is most frequently used:

$$\eta(\dot{\gamma}) = K\dot{\gamma}^{n-1} \tag{4}$$

The model contains two parameters, the consistency ($K$) and the power-law index ($n$). A value of $n = 1$ corresponds to Newtonian behavior; for shear thinning fluids $n < 1$. The simplest model that captures yield-stress behavior is the Bingham model used to describe viscoplastics:

$$\begin{aligned} \dot{\gamma} &= 0 \quad \text{for} \quad \tau < \tau_y \\ \tau &= \eta\dot{\gamma} + \tau_y \quad \text{for} \quad \tau \geq \tau_y \end{aligned} \tag{5}$$

This model allows no motion below the yield stress ($\tau_y$) and Newtonian flow behavior above $\tau_y$. Numerous other models have been proposed for various shapes of flow curves, discussions of which can be found in Macosko (1994), Barnes (1993), and Larson (1988).

Shear thickening is a form of non-Newtonian behavior that is observed much less frequently (Barnes, 1989). As its name implies, shear thickening involves an increase in viscosity over a range of shear rates. This can be seen from Figure 6-4d, where the viscosity begins to increase at a critical shear rate, $\dot{\gamma}_c$, until it reaches a maximum value at a shear-rate, $\dot{\gamma}_m$, following which it begins to drop. The viscosity increase typically occurs over a narrow range of shear-rates. This is in contrast to shear thinning, where the viscosity can decrease continuously over several decades of shear rate. Shear thickening phenomena are observed in a few concentrated colloidal dispersions and some polymer solutions.

In the examples given above, the flow curves represent equilibrium or steady-state behavior. Some materials, however, take a long time to reach steady state at constant shear,

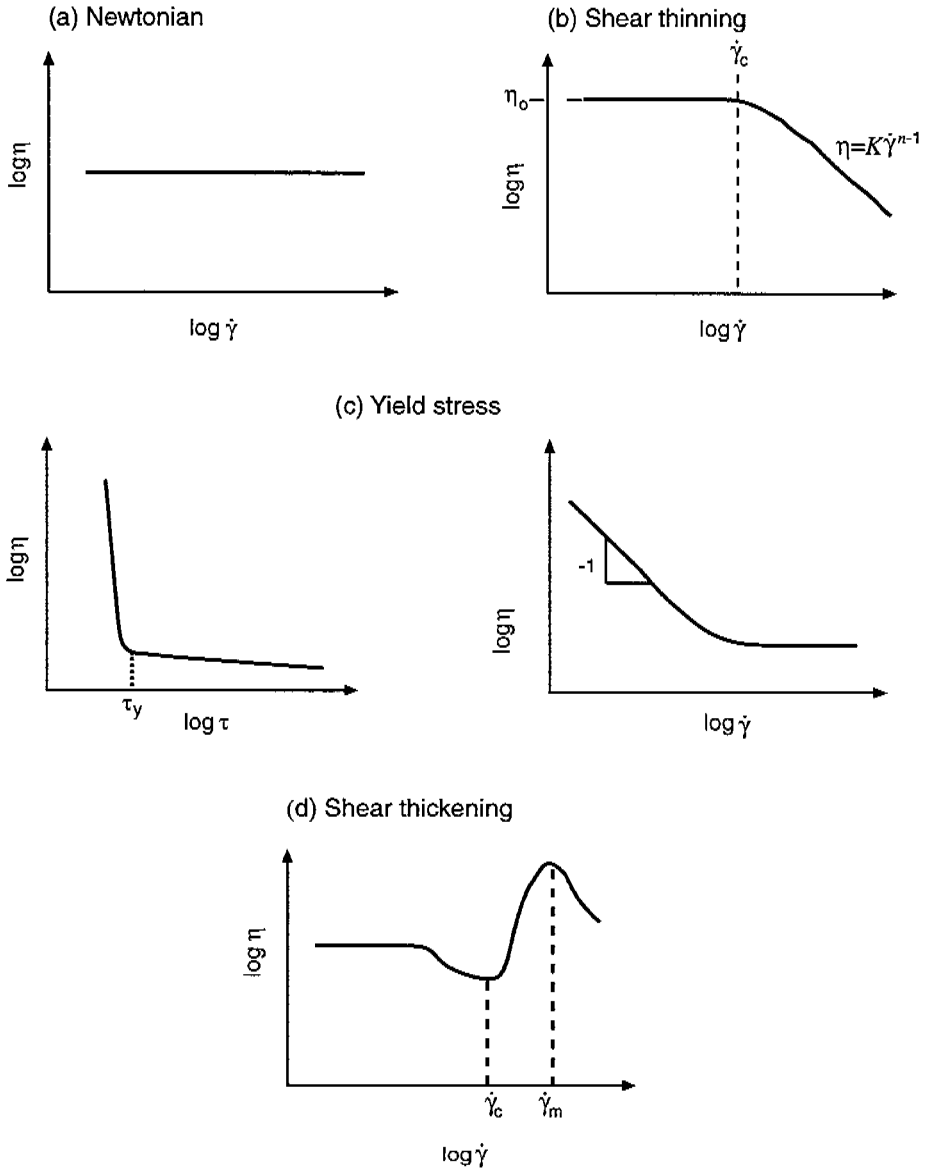


FIGURE 6-4 Examples of material behavior under steady shear (flow curves): (a) Newtonian; (b) shear thinning; (c) yield stress, shown in plots of viscosity vs. shear stress and shear rate; and (d) shear thickening.

i.e., their viscosity shows a continuous change with time of shear. The time-dependent phenomenon where the viscosity continuously decreases with time of shear is called *thixotropy* (Mewis, 1979). Thixotropic materials may also take considerable time to return to an at-rest state after being subjected to intense shear. These phenomena are widely observed in paints, adhesives, sealants, etc.

All rheological behavior, whether time-dependent or related to changes in shear, arises from changes in the microstructure of the system. This aspect will be a recurring theme in this paper. For example, consider a colloidal dispersion that shows yield stress and shear thinning. Such behavior typically signifies the presence of a particulate network structure in the system at rest and the shear-induced breakdown of the network into individual particles. The correlation between rheology and microstructure can be better understood after we discuss dynamic rheology and the linear viscoelastic response of different materials.

## DYNAMIC RHEOLOGY

In dynamic shear flow (also called oscillatory shear), a sinusoidally varying deformation (strain) is applied to the sample (Ferry, 1980):

$$\gamma = \gamma_0 \sin(\omega t) \tag{6}$$

where $\gamma_0$ is the strain-amplitude (i.e. the maximum applied deformation) and $\omega$ is the frequency of the oscillations. Figure 6-3b is a schematic representation of dynamic shear flow, and this can be compared to Figure 6-3a, which shows steady shear flow. The shear stress generated by the oscillatory shear will again be sinusoidal but will be shifted by a phase angle ($\delta$) with respect to the strain waveform:

$$\tau = \tau_0 \sin(\omega t + \delta) \tag{7}$$

Using trigonometric identities, the stress wave can be decomposed into two components, one in-phase with the strain and the other out-of-phase by 90 degrees:

$$\tau = \tau_0 \cos(\delta) \sin(\omega t) + \tau_0 \sin(\delta) \cos(\omega t) \tag{8}$$

We can rewrite the above expression in terms of two material functions ($G'$ and $G''$):

$$\tau = \gamma_0[G' \sin(\omega t) + G'' \cos(\omega t)] \tag{9}$$

Elastic or storage modulus, $$G' = \left(\frac{\tau_0}{\gamma_0}\right)\cos\delta \tag{10}$$

Viscous or loss modulus, $$G'' = \left(\frac{\tau_0}{\gamma_0}\right)\sin\delta \tag{11}$$

The elastic modulus ($G'$), which is related to the stress in phase with the imposed strain, provides information about the elastic nature of the material. Because elastic behavior implies the storage of deformational energy in the system, this parameter is also called the storage modulus. The viscous modulus ($G''$), on the other hand, is related to the stress component, which is completely out-of-phase with the displacement. This parameter characterizes the viscous nature of the material. Note that the out-of-phase component of the stress would be in phase with the sinusoidal deformation rate ($\dot{\gamma}$). Because viscous deformation results in the dissipation of energy, the $G''$ parameter is also called the loss modulus.

A purely elastic material would exhibit a non-zero elastic modulus and a viscous modulus $G'' = 0$. In contrast, a purely viscous material would show a show a zero elastic modulus, and its stress response would be 90 degrees out-of-phase with the strain ($\gamma$) and in-phase with the shear rate ($\dot{\gamma}$). A viscoelastic material will exhibit non-zero values for both $G'$ and $G''$. The above analysis assumes that the measurements are made in the "linear viscoelastic" (LVE) regime of the sample under consideration (Ferry, 1980). The conditions for linear viscoelasticity are that the stress be linearly proportional to the imposed strain and that the torque response involve only the first harmonic. The first condition requires that the moduli $G'$ and $G''$, in the LVE regime, should be independent of the strain-amplitude. The absence of higher harmonics in the stress response, as stipulated in the second condition, ensures that the response remains sinusoidal.

If these two conditions are met, the elastic and viscous moduli would truly be material functions. They would, however, be functions of the frequency of oscillation ($\omega$). A plot representing the moduli as a function of frequency, i.e., $G'(\omega)$ and $G''(\omega)$, is called the dynamic mechanical spectrum of the material. Such a plot is extremely useful because it represents a signature of the microstructure in the material. We can also define several auxiliary parameters based on the quantities derived above (Ferry, 1980). One such parameter is the complex viscosity ($\eta^*$), which is defined as:

$$\eta^* = \left[\left(\frac{G'}{\omega}\right)^2 + \left(\frac{G''}{\omega}\right)^2\right]^{1/2} \tag{12}$$

The variation of complex viscosity with frequency is analogous to the variation of steady viscosity versus shear-rate. (Note that both frequency and shear-rate have units of $s^{-1}$). Empirical correlation rules between the steady and complex viscosities, indicate a link between steady and dynamic rheology (Cox and Merz, 1958; Doraiswamy et al., 1991; Raghavan and Khan, 1997).

The two dynamic moduli $G'$ and $G''$ represent a clear distinction between elastic and viscous behavior in the same material. This helps to clarify the viscoelastic nature of a given sample. A simple model that captures the essential features of linear viscoelastic behavior is the Maxwell model, originally proposed by James Clerk Maxwell in 1867. In this model (shown in Figure 6-5), a viscoelastic sample is assumed to have two distinct elements: an elastic spring and a viscous dashpot connected in series (Macosko, 1994). The elastic spring has a shear-modulus ($G_0$), and the viscous component has a viscosity ($\eta_0$).

A characteristic parameter of a viscoelastic system is its *relaxation time* ($\lambda$), which in the case of the Maxwell model is equal to $\eta_0/G_0$. The relaxation time is a measure of the time required for stresses to relax in a viscoelastic material. Recall that under deformation, the stresses relax instantaneously for a viscous liquid; they never relax for an elastic solid. The Maxwell model is useful for simple viscoelastic systems, such as polymer solutions or melts, which exhibit a single relaxation time. We should mention that there are specific experiments to probe relaxation behavior, e.g., stress relaxation after a step strain, creep at constant stress, etc. A discussion of these experiments falls beyond the scope of this paper; details can be found in Bird et al. (1987), Ferry (1980) and Macosko (1994).

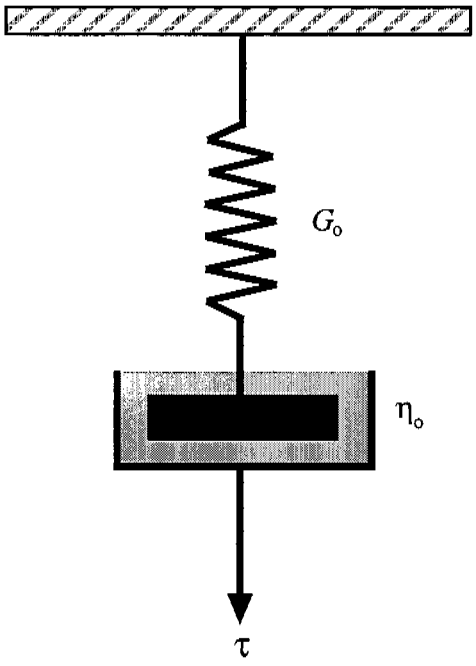


FIGURE 6-5 Maxwell model for a viscoelastic material. The system is considered to be a series combination of two distinct segments: an elastic spring (modulus $G_0$) and a viscous dashpot (viscosity $\eta_0$).

Perhaps the most important advantage of dynamic shear is that *it allows us to characterize microstructures without disrupting them in the process.* The net deformation imposed on the sample is minimal because the experiments are restricted to small deformations (strain amplitudes) within the LVE regime of the sample. As a result, the linear viscoelastic moduli reflect the microstructures present in the sample at rest. This is to be contrasted with steady shear, where the material functions are always obtained under flow conditions that correspond to relatively drastic deformations. Consequently, the microstructure under steady flow will be very different from the microstructure under static conditions. We can, therefore, correlate dynamic rheology to static microstructures and steady rheology to changes in microstructure caused by flow.

We will now illustrate the types of responses seen in dynamic frequency spectra, and furthermore, the correlation of these responses with material microstructure. We will also point out the steady-shear rheological behavior corresponding to these microstructures. Two classes of materials will be considered, colloidal dispersions and polymer melts. Colloidal dispersions are obtained by dispersing solid, colloidal-sized particles in a liquid (which, for simplicity, is assumed to be a purely viscous medium). The extent to which the particles flocculate depends on the strength of colloidal interaction forces between them (Russel et al., 1989). Various microstructures are thus possible, as illustrated in Figure 6-6.

In the simplest dispersions, inter-particle forces are negligible, i.e., each particle is discrete and does not "feel" the presence of its neighbors. These are classified as "non-flocculated" or stabilized dispersions. The typical dynamic rheological response of these systems (Figure 6-6a) consists of a dominant viscous modulus ($G''$) which exceeds the elastic modulus ($G'$) over the complete range of experimental frequencies (Macosko, 1994). The slopes of the $G'-\omega$ and $G''-\omega$ lines are often close to 2 and 1 respectively (note that frequency spectra are typically plotted in a log-log fashion as were the steady-shear flow curves). Under steady flow, the zero-shear viscosity of these dispersions will be relatively low, and the systems will show Newtonian or shear thickening behavior. (The concentration of solid particles has to be very high for shear thickening to occur). Note that the addition of colloidal particles always leads to an increase in viscosity over the pure liquid, but only a moderate increase is observed if the particles are non-interacting.

If the inter-particle forces are fairly strong, there will be a tendency for the particles to adhere to one another and form larger structures called aggregates or flocs (Mewis and Spaull, 1976). A flocculated microstructure is shown in Figure 6-6b along with its characteristic frequency spectrum. Note that $G'$ becomes larger than $G''$ at high frequencies but remains smaller at low frequencies. Both quantities show a weaker dependence on frequency, with lower slopes in the terminal zone (as compared to Figure 6-6a). Thus, dynamic rheology shows the viscoelastic nature of these systems as they exhibit comparable elastic and viscous character. The viscosity of a flocculated dispersion greatly exceeds the viscosity of a non-flocculated system. The steady-shear response is non-Newtonian and shear thinning, corresponding to the breakup of flocs into smaller and smaller units until they are reduced to individual particles.

Under conditions of strongly attractive inter-particle forces and high particle concentrations, flocculation of the system will be significant. Ultimately, the flocs will overlap with one another until a single floc fills the whole volume (Macosko, 1994). This corresponds to a situation where a three-dimensional network of particles extends throughout the system. A system containing a network-type microstructure is called a *gel.* The dynamic mechanical spectrum of a gel shows a frequency-independent elastic modulus ($G'$) that greatly exceeds the viscous modulus ($G''$) (Figure 6-6c). Thus, a gel behaves principally as an elastic material because of the presence of a continuous network. The level of elastic modulus ($G'$) can be correlated to the rigidity (i.e., the density of cross-links) in the network. In steady shear, a gel will show a yield stress at low shear, followed by shear thinning at higher shear rates. The yield stress signifies that a minimum stress is required to disrupt the cross-links in the network. Shear thinning reflects the progressive reduction in floc size as a result of shear.

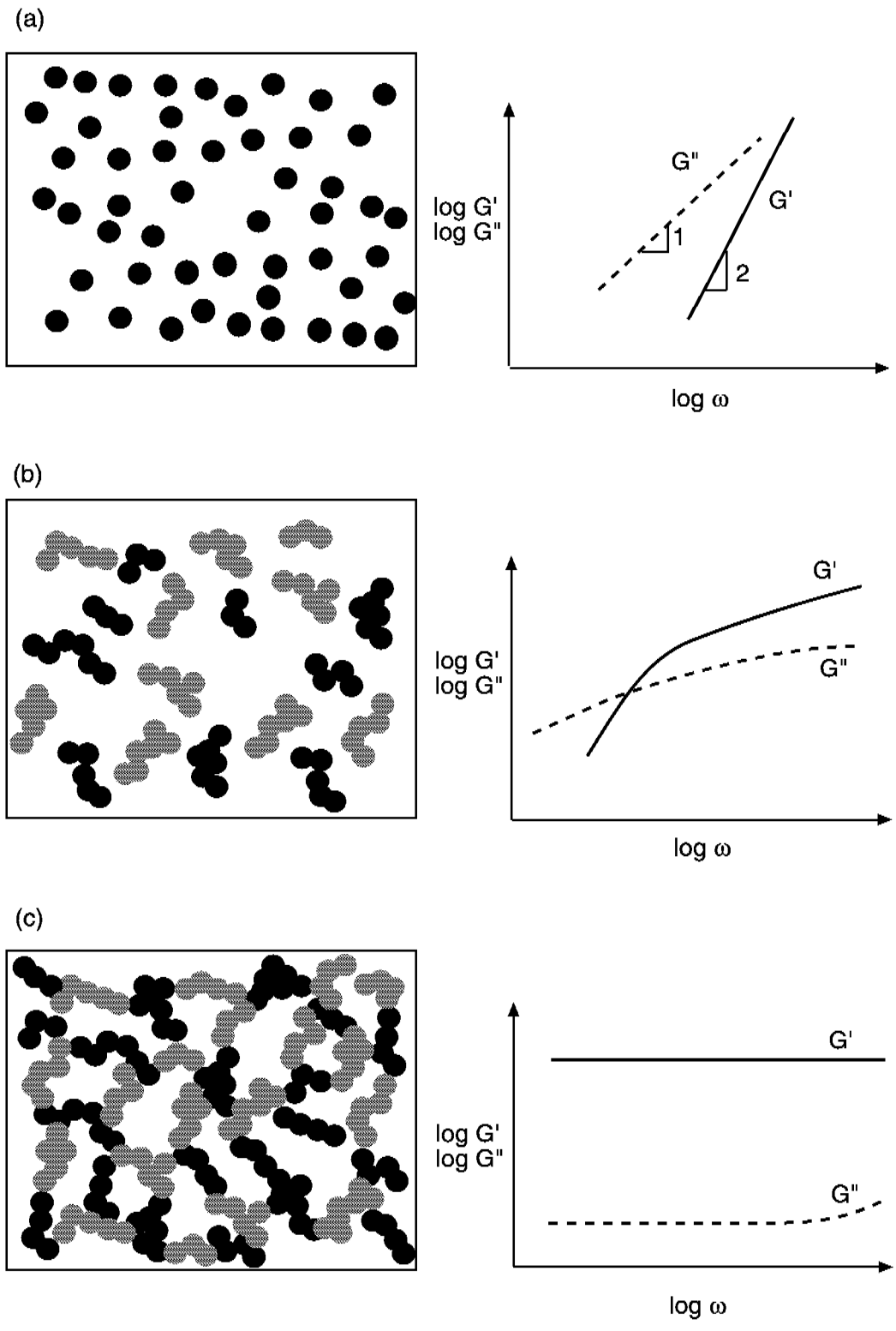


FIGURE 6-6 Dynamic rheology and microstructure of colloidal dispersions. In each case the frequency spectra ($G'$ and $G''$ as functions of frequency $\omega$) are shown with their corresponding microstructure. (a) Stabilized dispersion. (b) Weakly flocculated dispersion. (c) Strongly flocculated dispersion (gel).

We now consider the dynamic rheology of polymer melts over a range of molecular weights. This leads us to a consideration of "time-scales," a factor we largely ignored in the case of colloidal dispersions. Polymer melts can show very different behavior depending on the time-scales (or equivalently, the frequencies) probed in a rheological experiment (Dealy and Wissbrun, 1990). Note that low frequencies correspond to large time-scales and vice-versa. A typical rheological experiment may be conducted in the frequency range of $10^{-2}$ to $10^{2}$ rad/s, but data over a larger span of frequencies can be obtained by a procedure called time-temperature-superposition (TTS) (Ferry, 1980). This procedure utilizes the equivalence of time and temperature in the rheological context, i.e., dynamic rheological data obtained at higher temperatures is equivalent to data at longer time-scales (lower frequencies). Using TTS, we can generate data for a high molecular weight, monodisperse polymer melt over an extremely wide range of frequencies ($10^{-5}$ to $10^{4}$ rad/s), as illustrated schematically in Figure 6-7.

The plot shown in Figure 6-7 (note that both axes are on logarithmic scales) can be divided into three regions (Ferry, 1980). Region I corresponds to low frequencies (i.e., long time-scales) and is called the terminal region. It represents the frequency range that is experimentally accessible at any given temperature. We find that in the terminal zone both $G'$ and $G''$ increase steadily with frequency and the viscous modulus $G''$ is larger than the elastic modulus $G'$. The relations $G' \sim \omega^2$ and $G'' \sim \omega$ are typically found to be valid in this region, leading to slopes of 2 and 1 respectively for the lines. In Region II, the moduli cross over at a critical frequency, $\omega_c$, and $G'$ becomes greater than $G''$. The inverse of $\omega_c$ corresponds to the longest relaxation time for the polymer melt. The curves also begin to flatten and $G'$ plateaus off at a value given by $G_o^N$ (plateau modulus). Finally, in Region III, the moduli again increase with frequency, although to a smaller extent than in the terminal zone.

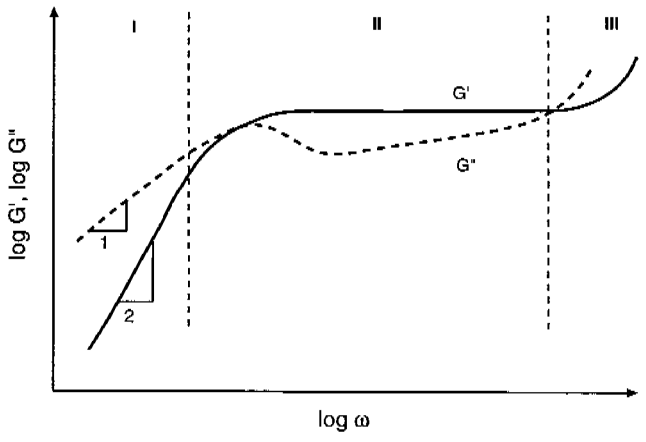


FIGURE 6-7 Dynamic mechanical spectrum ($G'$ and $G''$ as functions of frequency $\omega$) for a typical polymer melt over a wide range of frequencies (typically $10^{-3}$ to $10^{4}$ rad/s). The expanded frequency range is made possible by time-temperature-superposition (TTS). Region I is the terminal zone. Region II is the crossover/plateau region. Region III is the high-frequency regime.

The existence of a plateau in the frequency spectrum is caused by the presence of *entanglements* in the polymer melt. Entanglements can be envisioned as kinks in the polymer chain caused by segment to segment contacts with neighboring chains (Ferry, 1980; Macosko, 1994). The effect of entanglements is significant only for polymers with a molecular weight that exceeds the entanglement molecular weight ($M_e$). The length of the plateau region gives an indication of the extent of polymer chain entanglement. Thus, for a lower molecular-weight melt, the plateau region would be much smaller in width, and the crossover of $G'$ and $G''$ would occur at a higher frequency (smaller relaxation time).

The steady-shear rheology of a polymer melt is very sensitive to its molecular weight (Ferry, 1980; Bird et al., 1987). Low molecular weight melts are Newtonian liquids. As the molecular-weight increases, shear thinning begins to occur beyond a critical shear rate ($\dot{\gamma}_c$). The curves resemble the schematic shown in Figure 6-4b (and again in Figure 6-10) with a viscosity plateau ($\eta_0$) followed by shear thinning. As the molecular weight increases, shear thinning begins to set in at lower shear rates. From a microstructural point of view, shear thinning reflects a decrease in the density of entanglement with increasing shear because of progressive stretching and uncoiling of polymer chains (Ferguson and Kemblowski, 1991). An important trend in polymer rheology is the increase in zero-shear viscosity ($\eta_0$) with molecular weight (M) of the polymer melt (Ferry, 1980):

$$\begin{aligned} \eta_0 &= KM & M < M_e \\ \eta_0 &= KM^{3.4} & M > M_e \end{aligned} \qquad (13)$$

Thus, $\eta_0$ is initially proportional to the molecular weight but increases more sharply once the entanglement molecular weight ($M_e$) is exceeded. This indicates the critical role played by entanglements in polymer science.

## RHEOLOGICAL MEASUREMENTS (STEADY/ DYNAMIC SHEAR)

So far, we have indicated the two most important types of rheological techniques, i.e., steady shear and dynamic (oscillatory) shear. We have concentrated on a few important material functions, viz., the steady viscosity ($\eta$), and the dynamic moduli ($G'$ and $G''$). In this section, we briefly describe how these parameters are measured in practice. Rheological measurements are typically performed on a rheometer. There are several categories of rheometers, with the most prominent being capillary rheometers (which utilize

pressure-driven or Poiseuille flows) and rotational rheometers (which use drag flows). Capillary rheometers are capable of measuring only the steady-shear properties of a fluid, not the dynamic rheological properties. For this reason, we will focus solely on rotational instruments.

Two types of rotational rheometers exist: stress-controlled rheometers and strain-controlled rheometers (Ferguson and Kemblowski, 1991; Schramm, 1994). In a strain-controlled rheometer, a known deformation (strain or shear rate) is applied to the fluid, and the stress is detected. Typically, the strain is applied by rotating one segment of the geometry, and a transducer connected to the other segment measures the stress. A stress rheometer operates in the opposite fashion, by applying a controlled stress and measuring the resulting deformation. In the past few years, stress rheometers have become immensely popular because of their great sensitivity and wide torque range. Rotational rheometers also can use a multitude of different geometries. Concentric cylinder (Couette), parallel plates, and cone-and-plate are the most common geometries. For the purpose of illustration, we will consider the use of a cone-and-plate geometry on a strain-controlled rheometer and show how rheological quantities are calculated.

A schematic diagram of a cone-and-plate geometry is shown in Figure 6-8. The device consists of a small-angle cone and a flat plate. The cone angle is denoted to be $\alpha$, and the radius of the cone/plate is $R$. This geometry has several advantages: it requires only a small sample and is easier to load and clean than more complex geometries (Macosko, 1994). More importantly, a homogenous deformation is maintained throughout the sample, provided the cone angle is small (< 0.2 radians). Flow is generated in a rotational geometry by moving one of the walls of the system in such a way that the fluid is dragged along with the wall. This explains why these flows are called "drag flows" (Ferguson and Kemblowski, 1991).

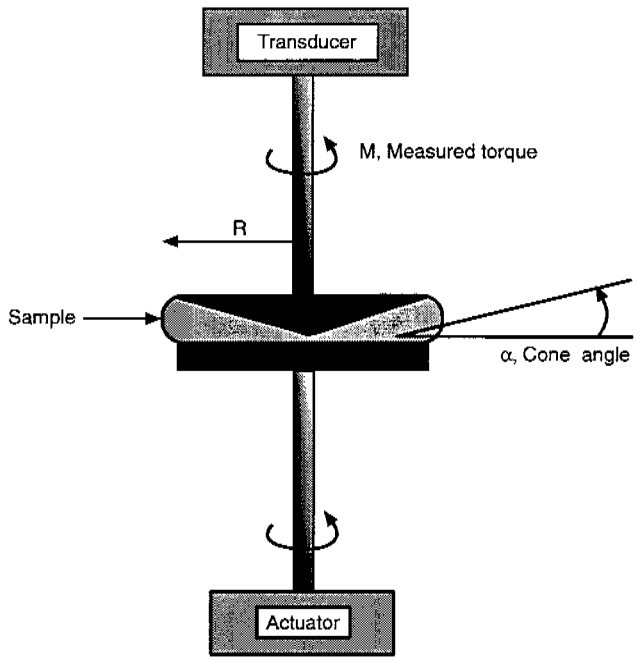


FIGURE 6-8 A rheological experiment on a cone-and-plate geometry on a strain-controlled rotational rheometer. The cone has a radius ($R$) and cone angle ($\alpha$), and its edge is truncated up to a height of 50 microns. The actuator applies a controlled deformation to the bottom plate, and the transducer connected to the cone measures the response of the sample.

In Figure 6-8 we show schematically how a test would be run on a cone-and-plate geometry using a strain-controlled rheometer. The general principle is to input a deformation and measure the torque output. The raw data can be converted into rheologically relevant quantities using the physical dimensions of the cone ($R$, $\alpha$) and the input parameters. Let us first consider a steady-shear experiment. In this case, the actuator rotates the bottom plate at an angular velocity $\Omega$ (rad/s). The shear-rate exerted on the sample is given by (Macosko, 1994):

$$\dot{\gamma} = \frac{\Omega}{\alpha} \tag{14}$$

The response of the sample is measured by the transducer in terms of a torque ($M$). The torque can be converted into a shear-stress ($\tau$) as follows:

$$\tau = \frac{3M}{2\pi R^3} \tag{15}$$

The apparent viscosity can then be calculated from the shear-stress and shear-rate by using the expression $\eta = \tau / \dot{\gamma}$. Thus,

$$\text{Apparent viscosity,} \quad \eta = \frac{3M\alpha}{2\pi R^3 \Omega} \tag{16}$$

In dynamic measurements, the bottom plate is oscillated from its mean position, with the peak displacement being up to an angle $\Phi$ (in radians). The strain-amplitude is then given by (Macosko, 1994):

$$\gamma_0 = \frac{\Phi}{\alpha} \tag{17}$$

The response of the sample is in terms of a sinusoidal torque showing a phase lag with respect to the input strain. The peak torque ($M$), and the phase angle ($\delta$), are measured by the instrument. The peak stress-amplitude ($\tau_0$) is calculated from the peak torque ($M$) using Eq. 15. The elastic and viscous moduli can then be calculated using Eqs. 9 and 10 respectively. The final expressions are:

$$\text{Elastic modulus,} \quad G' = \left(\frac{\tau_0}{\gamma_0}\right)\cos\delta = \frac{3M\alpha}{2\pi R^3 \Phi}\cos\delta \tag{18}$$

$$\text{Viscous modulus,} \quad G' = \left(\frac{\tau_0}{\gamma_0}\right)\sin\delta = \frac{3M\alpha}{2\pi R^3 \Phi}\sin\delta \tag{19}$$

Similar governing equations can be derived for other geometries (Macosko, 1994; Whorlow, 1992). It is important to note that these equations are obtained directly form the physical laws of motion. The rheological quantities calculated using these equations are, therefore, independent of any constitutive model.

## EXTENSIONAL RHEOLOGY

In the previous sections we considered steady-shear and dynamic shear, which are by far the most common types of rheological techniques. Most texts on rheology are devoted primarily to shear flow, and most laboratories are equipped only with shear rheometers. However, many viscoelastic phenomena are better perceived in extensional (elongational) flow, which is fundamentally different from shear flow. For simplicity, we will confine our discussion to steady uniaxial extension. (In the case of dynamic rheology, the type of deformation, i.e., shear versus elongation, is not important, because we consider only small deformations).

Uniaxial extension can be visualized to occur when a rod of fluid is gripped on each end and pulled (Figure 6-9) (Macosko, 1994; Dealy and Wissbrun, 1990). In the process, the sample is extended along the direction of imposed deformation and gets constricted along the two perpendicular directions. Thus, a cylindrical fluid element becomes longer and thinner as it is stretched. One of the main problems in extensional rheometry is the difficulty of achieving steady extensional flow, especially for low viscosity liquids. In discussing steady shear, we showed how a constant shear-rate could be imposed simply by moving the top plate at a constant velocity (v) (Figure 6-3a). However, to apply a constant elongation rate ($\dot{\varepsilon}$) the ends of the cylindrical sample shown in Figure 6-9 have to be moved at an exponentially-increasing velocity, given by (Macosko, 1994):

$$v_{end} = \frac{1}{2}\dot{\varepsilon} L_0 e^{\dot{\varepsilon} t} \qquad (20)$$

$L_0$ is the initial length of sample. The sample length ($L$) increases exponentially with time, while the area of the end-surface (A) decreases exponentially (assuming that the material is incompressible, so that the sample volume would not change). The stress causing the sample to elongate is the normal stress difference ($T_{xx} - T_{rr}$) which is the force ($f$) per unit area acting on the end of the sample. The extensional viscosity is obtained by dividing the normal stress by the elongation rate ($\dot{\varepsilon}$).

$$\text{Extensional viscosity,} \qquad \eta_e(\dot{\varepsilon}) = \frac{T_{xx} - T_{rr}}{\dot{\varepsilon}} = \frac{f/A}{\dot{\varepsilon}} \qquad (21)$$

From this discussion, we can appreciate the difficulties involved in designing an extensional rheometer, e.g., in designing clamps that move at an exponential pace to maintain a constant deformation. Other problems are the generation of a purely extensional flow free of shear effects and gravity effects. New rheometer designs (e.g. "opposing jets") are being developed to solve these problems (Macosko, 1994). Despite the difficulties, extensional rheology is worth studying for several reasons. Flows occurring in industrial processes, such as injection molding, extrusion, and calendering, often have a strong elongational component. Also, several viscoelastic phenomena including the tubeless siphon pointed out earlier are mainly elongational effects.

The behavior of a material under extension cannot be directly extrapolated from its behavior under shear. Consider the rheology of a polymeric melt under steady-shear as well as extension, as represented schematically in Figure 6-10. The steady-shear viscosity $\eta$ is constant at low shear rates and decreases at higher shear rates (shear thinning behavior). The extensional viscosity ($\eta_e$) is also a constant at low elongation rates, but $\eta_e$ increases at higher $\dot{\varepsilon}$. Within the regime of constant $\eta_e$, its value is three times the zero-shear viscosity ($\eta_0$).

$$\eta_e(\textit{at low } \dot{\varepsilon}) = \textit{constant} = 3\eta_0 \qquad (22)$$

This result, sometimes called Trouton's rule, was originally found by F.T. Trouton in 1906 and can be predicted from the continuum mechanics of the various flows. The increase in $\eta_e$ at higher deformations is called extensional-thickening and occurs for melts of polymers, such as polystyrene and low-density polyethylene. Thus, the same material can show shear

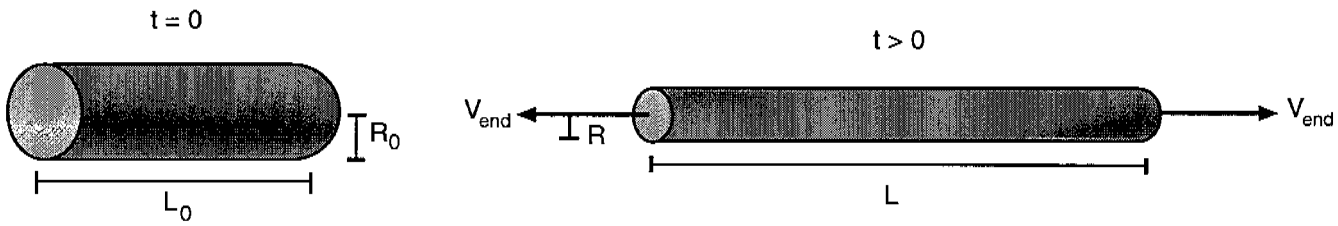


FIGURE 6-9 Uniaxial extensional flow on a cylindrical fluid element. Initially, the fluid is at rest, while at time $t > 0$, it is stretched by pulling the ends at a velocity ($v_{end}$). Note that the cylindrical sample becomes longer and thinner as it is stretched.

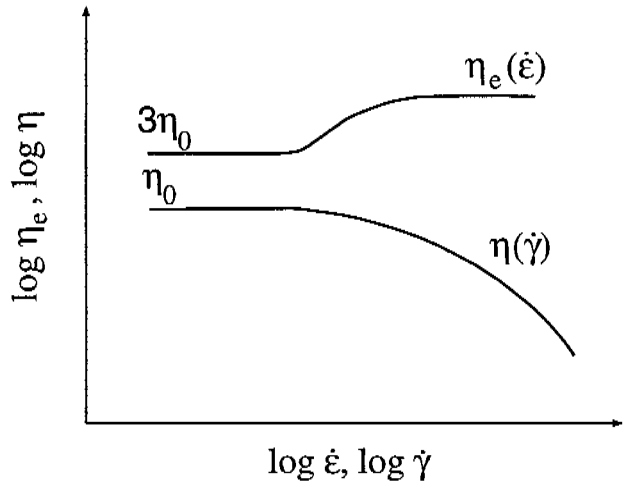


FIGURE 6-10 Typical behavior of a polymer melt under steady shear and steady uniaxial extension. Under steady shear the sample shows shear thinning; under extension it shows extensional thickening.

thinning under shear flow and extensional-thickening under elongational flow.

Extensional measurements can be more sensitive to small changes in the system composition than shear rheology. This is particularly true for polymer solutions containing very small amounts of polymer (in the 100 to 1000 ppm range), which show purely viscous behavior under shear and viscoelastic effects under extension (Chao et al., 1984). Similarly, solutions of associative polymers show anomalous effects that are much more pronounced under extension than under shear (Ballard et al., 1988).

## RHEOLOGY OF SILICA DISPERSIONS

In the next two sections, we provide a few examples of the use of rheology for characterizing and designing complex materials. We first consider the rheology of fumed-silica dispersions in oligomeric liquids, such as low molecular-weight glycols. These disperse systems have potential applications in state-of-the-art technologies, including "cable gels" for fiber-optic cables and composite polymer electrolytes for rechargeable lithium batteries (Khan et al., 1991; Khan and Zoeller, 1993). Colloidal dispersions can exhibit complex microstructures, as we pointed out in the previous section. The microstructure is a direct result of colloidal interactions between the particles, and therefore, varying the surface chemistry of the particles can have a significant effect on the microstructure. Because rheology is highly sensitive to microstructure, it is an invaluable tool for studying the origins of microstructural changes.

As an illustration, consider Figure 6-11 where we show the steady-shear rheology of two silica dispersions in the same liquid (a polypropylene glycol). Each dispersion has the same concentration of silica; the only difference is in the surface chemistry of each silica. One of the silicas (A200) is hydrophilic because of the presence of surface hydroxyl groups. This silica gives rise to a relatively low viscosity at low shear rates, and to shear thickening at higher shear rates. The other silica (R805) is hydrophobic, having an appreciable fraction of non-polar (octyl) surface groups. Its corresponding dispersion shows shear thinning over the entire range of shear-rates, and the viscosity at low shear rates is significantly higher than for the A200 silica dispersion.

In order to study the at-rest microstructures, we resort to dynamic rheological measurements. We show the elastic ($G'$) and the viscous ($G''$) moduli as a function of frequency in Figure 12 for the same systems shown in Figure 6-11. For the A200 (hydrophilic) silica dispersion, the viscous modulus ($G''$) is greater than $G'$ over the entire frequency range. Moreover, both moduli depend strongly on frequency. This signifies a non-flocculated microstructure composed of distinct particles (Figure 6-6a). In contrast, for the R805 (hydrophobic) silica dispersion, the moduli are independent of frequency, and the elastic modulus ($G'$) exceeds $G''$ over the entire frequency range. This frequency spectrum signifies that the latter system is a flocculated gel with a three-dimensional network structure.

We can form a picture of the colloidal interactions present in each dispersion by considering the steady and dynamic responses together. The A200 (hydrophilic) silica exists as

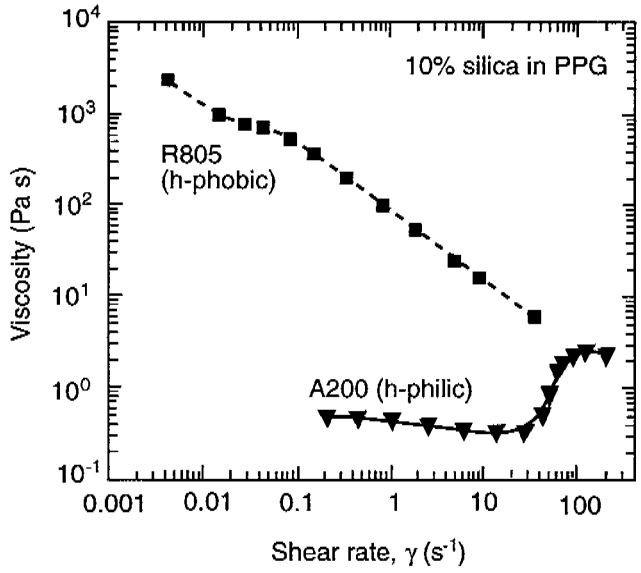


FIGURE 6-11 Steady shear viscosity ($\eta$) as a function of shear rate for two colloidal dispersions. Each dispersion contains 10 percent fumed silica in a poly(propylene glycol) of molecular weight 425 g/mol. The two silicas differ only in their surface chemistry, with one of them being hydrophilic and the other hydrophobic.

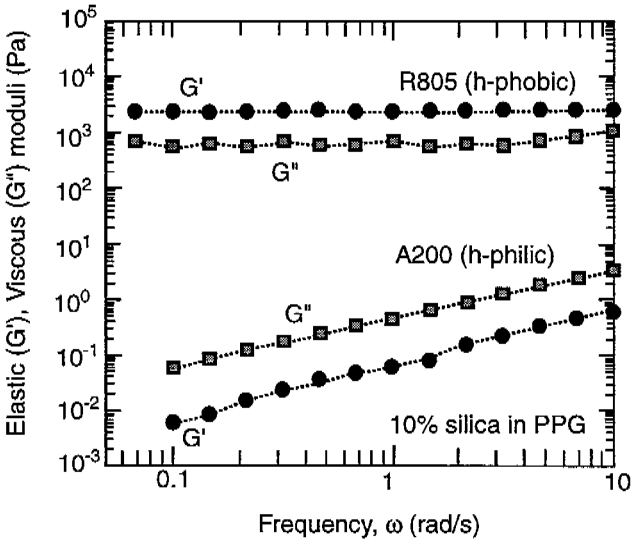


FIGURE 6-12 Elastic ($G'$) and viscous ($G''$) moduli as a function of frequency for the fumed-silica dispersions shown in Figure 6-11.

isolated particles that exhibit little or no tendency for flocculation. Consequently, the system behaves like a viscous fluid, as evidenced by the dominant $G''$ in its frequency spectrum (Figure 6-12) as well as its low zero-shear viscosity (Figure 6-11). It appears that the hydrophilic A200 surface preferentially interacts through hydrogen bonding with the polar groups present on the glycol, leading to steric stabilization of the particles (Raghavan and Khan, 1997). This contributes to an effective repulsive interaction between the particles, which acts as a barrier to flocculation. In contrast, the non-polar groups present on the R805 (hydrophobic) silica can interact with each other through van der Waals dispersion forces (Raghavan and Khan, 1995). This leads to the flocculation of silica particles, as shown by a pronounced elastic response in the dynamic data (Figure 6-12) and high viscosities under steady shear (Figure 6-11). The shear thinning of the R805 dispersion is caused by progressive reduction in floc size due to shear.

We would also like to comment briefly on the microstructural origins of shear thickening. This is a reversible flow-induced phenomenon where the viscosity increases under flow but where the system reverts back to its low-viscosity state at rest (Barnes, 1989). Current experimental and theoretical investigations have confirmed that shear thickening is caused by the formation of temporary clusters under flow (Raghavan and Khan, 1997). These "hydrodynamic clusters" are formed by the action of hydrodynamic forces that squeeze particles together into larger groups (Bossis and Brady, 1989). In order for these clusters to be formed, the hydrodynamic forces (which increase steadily with shear-rate) first have to overcome the steric repulsion forces. Therefore, shear thickening occurs only beyond a critical shear rate, as seen in Figure 6-11.

## RHEOLOGY OF ASSOCIATIVE-POLYMER SOLUTIONS

We now proceed to consider the rheology of polymeric systems formed by dissolving an "associative polymer" in water. An associative polymer is typically a water-soluble polymer that also possesses hydrophobic groups (Hansen et al., 1996). Small amounts of these polymers can greatly increase the viscosity of aqueous media, due to strong interactions between the hydrophobic groups. Thus the concentration, type, and length of the hydrophobic moiety are important in determining the properties of the system. In our laboratories, we have done extensive work on aqueous solutions of hydrophobically modified alkali-soluble emulsion (HASE) polymers. These polymers possess a comb-like structure, with pendant hydrophobic groups sticking out of the polymer backbone (English et al., 1997a).

We will briefly look at two effects, polymer concentration and the presence of surfactants. In Figure 6-13, we show steady-shear data (viscosity as a function of shear-stress) for aqueous solutions containing different polymer concentrations. As the concentration is increased from 0.4 to 1.0 g/dl, the zero-shear viscosity ($\eta_0$) increases by a factor of 1000. In fact, if we plot $\eta_0$ versus polymer concentration ($c$) we find that ($\eta_0 \sim c^8$, a much more dramatic increase than for regular polymers, for which $\eta_0 \sim c^{3.4}$ (scaling similar to the variation of $\eta_0$ with melt molecular weight). Note also that there are basic differences between the shapes of the viscosity curves at low concentrations and high concentrations. At low concentrations, the initial Newtonian plateau is followed by an intermediate range of mild shear thickening and then a region of drastic shear thinning. At high concentrations, the shear thickening is no longer observed but a viscosity plateau exists at intermediate stresses. Also, the viscosity drops abruptly by

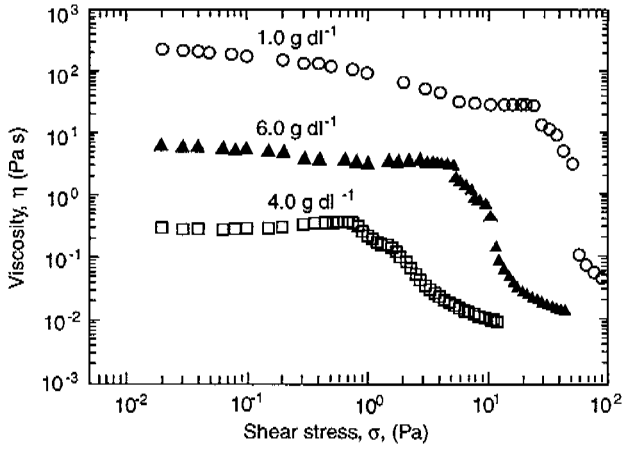


FIGURE 6-13 Steady shear viscosity ($\eta$) as a function of shear stress for aqueous solutions of an associative polymer. Data is shown for three different polymer concentrations.

orders of magnitude at a higher stress(behavior reminiscent of a pseudo yield-stress.

Clearly, the rheology of associative polymer solutions is much more complex than the simple cases we have considered thus far. This is because hydrophobic interactions can be either intrapolymeric (between hydrophobes on the same chain) or interpolymeric (between hydrophobes on adjacent chains), with a combination of both mechanisms at any given stress level. We believe that the dominant mode of interaction is intrapolymeric at low stresses and interpolymeric at intermediate stresses (English et al., 1997). The interpolymeric interactions contribute to shear thickening and to the viscosity plateau (Ballard et al., 1988). At very high stresses, all hydrophobic interactions are precluded, as the hydrodynamic forces in the system begin to dominate. The transition from a state of appreciable interactions to negligible interaction occurs at the pseudo yield-stress.

Another significant effect in these systems is caused by the presence of surfactant. Consider an aqueous solution of HASE polymer at a polymer concentration of 0.6 g/dl (Figure 6-14). The elastic modulus ($G'$) for this system varies with frequency as $\omega^{0.8}$ (at low $\omega$) and exceeds the viscous modulus ($G''$) only at high frequencies. When we add 1.5 g/dl of a non-ionic surfactant to the system, we find that the levels of both $G'$ and $G''$ are increased. Moreover, the elastic modulus ($G'$) shows plateau-like behavior over most of the frequency range and is higher than the viscous modulus ($G''$) over the entire spectrum. This indicates that the addition of surfactant renders the system more elastic. We conjecture that this behavior is caused by enhanced hydrophobic interaction in the system, with the surfactant molecules acting as links between polymer hydrophobes. Note that the molecular structure of the surfactant is crucial to its behavior; other types of surfactants can produce the reverse effect, i.e., they can reduce the elastic character of the system.

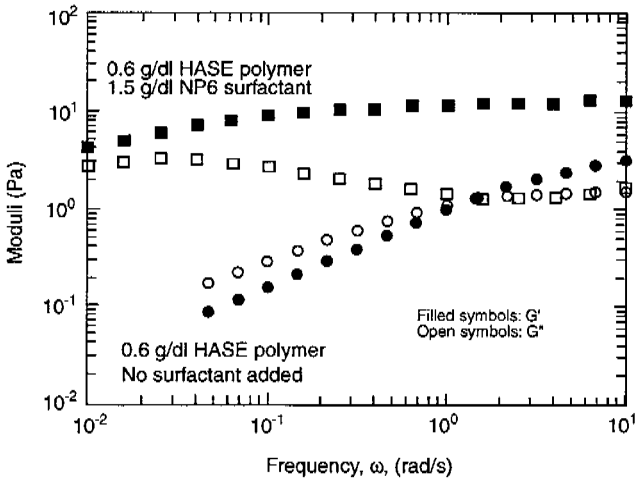


FIGURE 6-14 Elastic ($G'$) and viscous ($G''$) moduli as a function of frequency for two associative polymer solutions. In one system only polymer is present; the other contains 1.5 g/dl of a non-ionic surfactant (NP6) in addition to polymer. The steady-shear data for the polymer solution in the absence of surfactant was shown in Figure 6-13.

## RHEOLOGY OF AVIATION FUELS

Currently, the fuels used in the gas-turbine engines of commercial aircraft are kerosene-based jet fuels (Hutchinson, 1995). The two main types are Jet A fuel, used in North America, and Jet A-1, used in most other regions of the world. Jet fuels are among the most tightly specified products of oil refineries, the specifications involving boiling point, water content, aromatic content, etc. The important qualities jet fuels must generally exhibit under all operating conditions are as follows (Kroes and Wild, 1995):

- pumpability and ease of flow, with negligible volatility
- efficient combustion and high calorific value
- adequate lubrication for the moving parts of the engine
- minimal corrosive effects, fire hazards, etc.

The viscosity of an aviation fuel is a factor in calculating pressure drops in fuel lines, through its relationship to the Reynolds number (Bird et al., 1987). A lower viscosity corresponds to smaller pressure drops and lower pumping requirements. The viscosity increases with decreasing temperature, and when the freezing point of the fuel is approached, waxy particles begin to form. Many fuel specifications, therefore, include a maximum viscosity limit at low temperatures to ensure pumping and flow capabilities (CRC report, 1984). Research on aviation fuels has also led to the development of additives for specific purposes, e.g. to prevent ice and bacterial contamination in the fuel or to reduce the buildup of static charge (Kroes and Wild, 1995).

One class of additives is intended to reduce the flammability of aviation fuels in the event of an accident or crash. These additives, called "antimisting" (AM) agents, are essentially linear polymers of high molecular weight ($> 10^6$) (Chao et al., 1984). A small amount of polymeric additive (100 ppm) is sufficient to reduce the formation of atomized droplets or "mist." Droplets in sprays of antimisting fuels tend to be larger and, in some cases, deformed to strings or filaments (Hoyt et al., 1980). The reduction of surface area available for vaporization, combined with the greater distance between droplets, inhibits flame propagation.

The antimisting behavior of fuels containing polymeric additives is a consequence of the viscoelastic nature of the fuel system (Hoyt et al., 1980; Chao et al., 1984). Accordingly, it is important to study the rheology of AM fuels. Under shear flow, however, non-Newtonian effects cannot

be detected for these systems because of the low level of polymer concentrations. On the other hand, the appearance of filaments in antimisting fuel sprays is an indication that there is a strong elongational component in spray hydrodynamics. This points to the significance of extensional rheology in AM fuels. Chao et al. (1984) attempted to correlate the extensional viscosity ($\eta_e$) of the fluid to its antimisting behavior. They resorted to an indirect, yet simple and inexpensive indicator of $\eta_e$, viz., the ductless siphon height. The height ($h^*$) to which a viscoelastic fluid can raise itself in the absence of an immersed duct (see Figure 6-2) can be taken as a measure of the fluid's extensional viscosity ($\eta_e$). The researchers found that AM fuels showing large values of the ductless siphon height ($h^*$), and thereby $\eta_e$, also exhibited strong antimisting behavior. Moreover, as the polymer molecular weight or concentration in solution was increased, the fuel became more viscoelastic (greater h*), and the antimisting action was enhanced.

One of the penalties of using polymeric additives in fuels is the increased viscosity of the system (Chao et al., 1984). It should be noted that large increases in fuel viscosity caused by additives is undesirable because it increases pumping requirements, and affects the temperature at which the viscosity exceeds specifications. Thus, care must be taken in selecting polymeric materials to be added to jet fuels. The study by Chao et al. (1984) found that using a high molecular-weight polymer, for which kerosene was an extremely good solvent, is desirable. If such a polymer was used at a low concentration, the viscosity increase could be kept within manageable limits, and antimisting properties would be conferred to the fuel.

This example illustrates the utility of rheology for aviation fuel research, especially for systems that are rendered non-Newtonian or viscoelastic by additives. Future research on aviation fuels might involve designing new additives and considering alternate fuels to prevent fire in "survivable" crashes. Possible additives are combinations of associative polymers and surfactants to produce materials with "tunable" properties. Very small amounts of these materials may be sufficient to produce changes in fuel rheology. Furthermore, one can obtain different rheological behavior depending on the operating regimes (cf. Figure 6-13, where the viscosity varies in a complex manner with shear-rate). Thus, we expect rheology to play a greater role in the design of the next generation of aviation fuels.

## SUMMARY

In this paper, we have presented a primer on rheology, the science of flow and deformation in various kinds of matter. We showed that rheologically interesting materials do not obey either Newton's law of viscosity or Hooke's law of elasticity; instead they can be classified as "viscoelastic," i.e., they exhibit a combination of viscous and elastic properties. Most colloidal and macromolecular systems fall into this category.

We considered three rheological methods: steady shear, dynamic oscillatory shear, and extensional flow. The most important material parameters obtained using these methods were outlined, viz., the steady-shear viscosity ($\eta$), the elastic ($G'$) and viscous ($G''$) moduli in the linear viscoelastic regime of dynamic shear, and the extensional viscosity ($\eta_e$). We showed how these parameters can be correlated to the underlying microstructure of various materials. Finally, we also discussed an example of how rheology could be used to evaluate polymeric additives for aviation fuels. On the whole, we hope to have shown the utility and efficacy of rheology for characterizing condensed matter.

## REFERENCES

Ballard, M.J., R. Buscall, and F.A. Waite. 1988. The theory of shear thickening polymer solutions. Polymer 29:1287–1293.

Barnes, H.A. 1989. Shear thickening (dilatancy) in suspensions of nonaggregating solid particles dispersed in Newtonian liquids. Journal of Rheology 33:329–366.

Barnes, H.A. 1993. Rheology for the chemical engineer. The Chemical Engineer June 24:17–23.

Bird, R.B., R.C. Armstrong, and O. Hassager. 1987. Dynamics of Polymeric Liquids, Vol. 1: Fluid Mechanics (2nd ed). New York: Wiley and Sons.

Boger, D.V., and K. Walters. 1993. Rheological Phenomena in Focus. Amsterdam: Elsevier.

Bossis, G., and J.F. Brady. 1989. The rheology of Brownian suspensions. Journal of Chemical Physics 91:1866–1874.

Chao, K.K., C.A. Child, E.A. Grens, and M.C. Williams. 1984. Antimisting action of polymeric additives in jet fuels. American Institute of Chemical Engineering Journal 30(1):111–120.

CRC Report No. 530. 1984. Handbook of Aviation Fuel Properties. Atlanta, Ga.:Coordinating Research Council.

Dealy, J.M., and K.F. Wissbrun. 1990. Melt Rheology and Its Role in Plastics Processing. New York: Van Nostrand Reinhold.

Doraiswamy, D., A.N. Majumdar, I. Tsao, A.N. Beris, S.C. Danforth, and A.B. Metzner. 1991. The Cox-Merz rule extended: A rheological model for concentrated suspensions and other materials with a yield stress. Journal of Rheology 35(4):647–685.

English, R.J., H.S. Gulati, R.D. Jenkins, and S.A. Khan. 1997. Solution rheology of a hydrophobically-modified alkali soluble associative polymer. Journal of Rheology 41:427–444.

Ferguson, J., and Z. Kemblowski. 1991. Applied Fluid Rheology. London:Elsevier.

Ferry, J.D. 1980. Viscoelastic Properties of Polymers (3rd ed). New York: Wiley and Sons.

Hansen, F.K., B. Nystrom, and H. Walderhaug. 1996. Associating polymers: Introduction. Colloids and Surfaces A 112:85–89.

Hoyt, J.W., J.J. Taylor, and R.L. Altman. 1980. Drag reduction-jet breakup correlation with kerosene-based additives. Journal of Rheology 24(5):685–699.

Hutchinson, J. 1995. Aviation fuel: A subject of intense research and development. Aircraft Engineering and Aerospace Technology 67(2):10–12.

Khan, S.A., M.A. Maruca, and I.M. Plitz. 1991. Rheology of fumed silica dispersions for fiber-optic cables. Polymer Engineering and Science 31:1701–1707.

Khan, S.A., and N.J. Zoeller. 1993. Dynamic rheological behavior of flocculated fumed silica suspensions. Journal of Rheology 37:1225–1235.

Khan, S.A., G.L. Baker, and S. Colson. 1994. Composite polymer electrolytes using fumed silica fillers: Rheology and ionic conductivity. Chemistry of Materials 6:2359–2363.

Kroes, M.J., and T.W. Wild. 1995. Aircraft powerplants. New York: McGraw-Hill.

Larson, R.G. 1988. Constitutive Equations for Polymer Melts and Solutions. Boston: Butterworth.

Macosko, C.W. 1994. Rheology: Principles, Measurements, and Applications. New York: VCH Publishers.

Mewis, J. 1979. Thixotropy: A general review. Journal of Non-Newtonian Fluid Mechanics 6(1):1–20.

Raghavan, S.R., and S.A. Khan. 1995. Shear-induced microstructural changes in flocculated suspensions of fumed silica. Journal of Rheology 39(6):1311–1325.

Raghavan, S.R., and S.A. Khan. 1997. Shear thickening response of fumed silica suspensions under steady and oscillatory shear. Journal of Colloid and Interface Science 185:57–67.

Russel, W.B., D.A. Saville, and W.R. Schowalter. 1989. Colloidal Dispersions. Cambridge, U.K.: Cambridge University Press.

Schramm, G. 1994. A Practical Approach to Rheology and Rheometry. Karlsruhe, Germany: Gebrueder HAAKE GmbH.

Whorlow, R.W. 1992. Rheological Techniques (2nd ed). London: Ellis Horwood.